

Long-Chain Polyorthoesters as Degradable Polyethylene Mimics

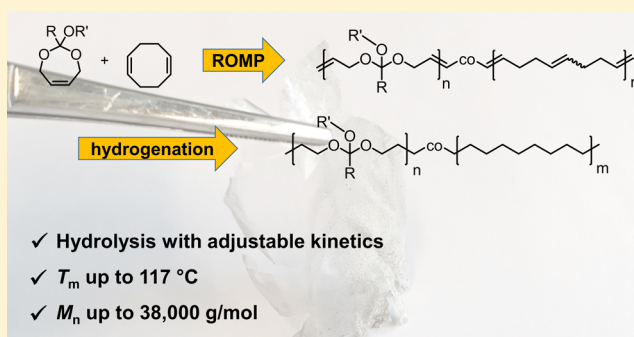
Tobias Haider,[†] Oleksandr Shyshov,[‡] Oksana Suraeva,[†] Ingo Lieberwirth,[†] Max von Delius,[‡] and Frederik R. Wurm^{*†}

[†]Max Planck Institute for Polymer Research, Ackermannweg 10, 55128 Mainz, Germany

[‡]Institute of Organic Chemistry and Advanced Materials, University of Ulm, Albert-Einstein-Allee 11, 89081 Ulm, Germany

Supporting Information

ABSTRACT: The persistence of commodity polymers makes the research for degradable alternatives with similar properties necessary. Degradable polyethylene mimics containing orthoester groups were synthesized by olefin metathesis polymerization for the first time. Ring-opening metathesis copolymerization (ROMP) of 1,5-cyclooctadiene with four different cyclic orthoester monomers gave linear copolymers with molecular weights up to 38000 g mol⁻¹. Hydrogenation of such copolymers produced semicrystalline polyethylene-like materials, which were only soluble in hot organic solvents. The crystallinity and melting points of the materials were controlled by the orthoester content of the copolymers. The polymers crystallized similar to polyethylene, but the relatively bulky orthoester groups were expelled from the crystal lattice. The lamellar thickness of the crystals was dependent on the amount of the orthoester groups. In addition, the orthoester substituents influenced the hydrolysis rate of the polymers in solution. Additionally, we were able to prove that non-hydrogenated copolymers with a high orthoester content were biodegraded by microorganisms from activated sludge from a local sewage plant. In general, all copolymers hydrolyzed under ambient conditions over a period of several months. This study represents the first report of hydrolysis-labile and potentially biodegradable PE mimics based on orthoester linkages. These materials may find use in applications that require the relatively rapid release of cargo, e.g., in biomedicine or nanomaterials.



1. INTRODUCTION

Today polyethylene (PE) is the most used commodity polymer in the world.¹ Because of its excellent mechanical properties, PE is used for a variety of applications.² However, there are environmental issues related to the low degradability of PE in the environment. Increasing plastic pollution in natural environments amplifies the need for degradable alternatives.³

To mimic the properties of polyethylene while potentially enabling degradation at the same time, one approach lies in the incorporation of functional groups in long aliphatic polymer chains.⁴ Among others, long-chain polyesters,⁵ polyamides,⁶ polyketones,⁷ or polyphosphoesters⁸ have been reported. There, the functional groups act as “defects” in the polymer chains of the semicrystalline materials. Depending on their size, the defects are either part of the lamellar PE crystals (small defect size) or forced into the amorphous phase (bulky defects).⁹ An increasing number of methylene units between the functional groups enhances van der Waals interactions between the polymer chains, leading to a higher degree of crystallinity.⁴ As a result, hydrophobicity, melting temperature, and stiffness of the material increase.⁴ Yet, concerning degradability, long-chain polyesters, for example, did not show relevant enzymatic or hydrolytic degradation as water is

hindered from penetrating into the materials due to the high crystallinity and hydrophobicity.⁴ Also, long chain polyacetals revealed only minor degradation in acidic media.¹⁰ Thus, the use of functional groups, which are more prone to hydrolysis, is advisable. Similar to acetals in molecular structure, but with a higher hydrolysis rate¹¹ and steric bulk, orthoesters can be a suitable alternative to synthesize acid-sensitive polymers.

Acid-degradable polymers are also attractive for drug delivery;¹² polyorthoesters were developed in the 1970s by the group of Jorge Heller for biomedical applications.^{13–16} The hydrolysis of polyorthoesters in acidic media yields alcohols and esters (Scheme 1), while the degradation of the bulk material was shown to proceed via surface erosion.¹⁵

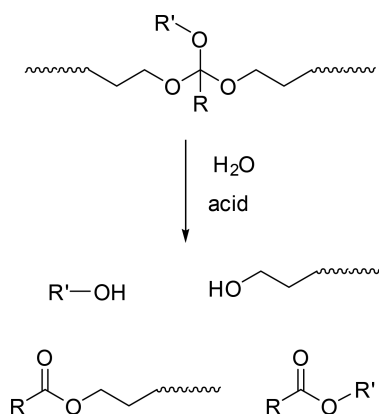
While polyacetals were synthesized by acyclic diene metathesis (ADMET) polymerization,^{17,18} ring-opening metathesis copolymerization (ROMP),¹⁹ or polycondensation,²⁰ polyorthoesters are mainly prepared either through transesterification of orthoesters with diols or through polyaddition between a diol and a diketene acetal (Scheme 2).²¹

Received: January 24, 2019

Revised: February 27, 2019

Published: March 13, 2019

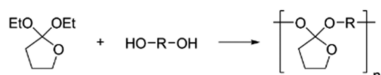
Scheme 1. Hydrolysis of Polyorthoesters to Alcohols and Esters



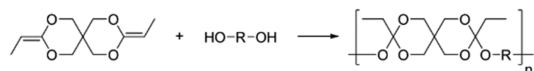
Scheme 2. Synthesis Methods for Polyorthoesters

J. Heller:

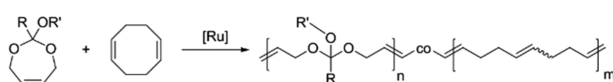
Transesterification



Polyaddition

**This work:**

ROMP



Dove et al. reported the synthesis of different polyorthoesters by polyaddition using bifunctional, air- and moisture-stable vinyl acetal precursors.²² In general, the mechanical and thermal properties of polyorthoesters can be adjusted by varying the structure of the monomers (mainly the diols). By changing the hydrophobicity of the polymer, the degradability of the material can be tuned. However, this requires the use of new, different monomers if the polymerization is conducted by transesterification or polyaddition. Recently, von Delius and co-workers explored the use of orthoesters for the self-assembly of novel supramolecular hosts^{23–25} and in this context demonstrated that the degradation rate of orthoesters strongly depends on the orthoester substituent (R group in Scheme 1): electron-rich orthoesters (R = $-\text{CH}_3$) hydrolyze even at neutral pH, while more electron-deficient orthoesters (R = $-\text{CCl}_3$) are remarkably stable.²⁶ For drug delivery applications, von Delius recommend the use of orthoformates (R = $-\text{H}$) and chloromethyl-substituted orthoesters (R = $-\text{CH}_2\text{Cl}$) based on observed hydrolysis half-lives of 20 and 120 min at pH 5, respectively.

In this work, we present a straightforward approach to long-chain polyorthoesters by performing for the first time a ring-opening metathesis copolymerization of cyclic orthoesters with 1,5-cyclooctadiene followed by exhaustive hydrogenation. By the variation of the comonomer ratio, the number of methylene groups between two orthoester units can be controlled. Monomers featuring three different orthoester substituents were studied based on the hypothesis that the

corresponding polymers would differ in hydrolysis rate. The thermal and mechanical properties of the polyethylene-like polymers were studied as well as the degradation in an organic solvent and in aqueous media.

2. RESULTS AND DISCUSSION

Monomer Synthesis. Starting from the corresponding orthoesters trimethyl orthoacetate, trimethyl orthoformate, triisopropyl orthoformate, and 2-chloro-1,1,1-trimethoxyethane, we synthesized four different cyclic orthoester monomers (1–4) by reacting the respective starting compounds with *cis*-2-butene-1,4-diol under acidic catalysis (Scheme 3A). Moisture had to be strictly excluded during these procedures, as it would lead to hydrolysis of the orthoester. The monomers were purified by (repeated) distillation to yield colorless oils.

Ring-Opening Metathesis Polymerization. The cyclic orthoester monomers are seven-membered and substituted 4,7-dihydro-1,3-dioxepins (Scheme 3) with a substitution at the C2. In previous works, Kilbinger and co-workers synthesized polyacetals as sacrificial blocks to prepare telechelic polynorbornenes using dioxepins.²⁷ Grubbs et al. reported the ROMP of 4,7-dihydro-1,3-dioxepine and phenyl-substituted 4,7-dihydro-2-phenyl-1,3-dioxepin to polyacetals.¹⁹ However, they were able to prove that only the unsubstituted dioxepin underwent successful homopolymerization. In contrast, we were able in previous work to produce homopolymers of phosphorus-containing seven-membered rings, namely 2-phenoxy-4,7-dihydro-1,3,2-dioxaphosphepine 2-oxide²⁸ and 2-methyl-4,7-dihydro-1,3,2-dioxaphosphepine 2-oxide.⁸

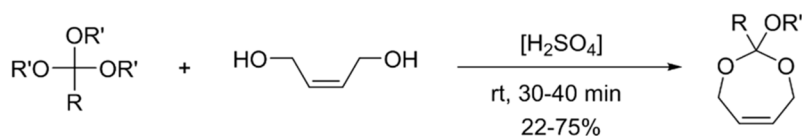
To date, no polyorthoesters have been reported by metathesis polymerization. In accordance with previous studies, the attempted homopolymerization of the orthoester monomers 1 and 2 did not yield any polymers, even if catalyst type and conditions were varied (cf. Table S1).

During ROMP, the release of ring strain of the cyclic olefin is the driving force of the polymerization.²⁹ The unsubstituted dioxepin, however, already exhibits relatively low ring strain. Further substituents hinder the ROMP due to the Thorpe–Ingold effect: substituents on a ring stabilize the ring-closed form relative to the linear counterpart. With ROMP being an equilibrium process, the Thorpe–Ingold effect results in a higher critical monomer concentration. This leads to a lower yield of the linear polymer—or to no polymer at all.^{30–32} However, monomers with low ring strain can be activated by a more active comonomer: the copolymerization of 1,5-cyclooctadiene (COD) with an unsubstituted or a methyl-substituted 4,7-dihydro-1,3-dioxepins gave statistical COD/dioxepin copolymers.¹⁹ Thus, we followed this approach to copolymerize our four cyclic orthoester monomers with COD using a first-generation Hoveyda–Grubbs catalyst as the initiator (0.4 mol % relative to the total amount of comonomers). The polymerizations were conducted in bulk at room temperature overnight, yielding polymers with apparent molecular weights up to 38000 g mol⁻¹ (by SEC vs polystyrene standard). Monomers 1–4 were transformed successfully into copolymers with different amounts of orthoesters incorporated into the polymer chain, which controls the chain length of the degradation products (Table 1).

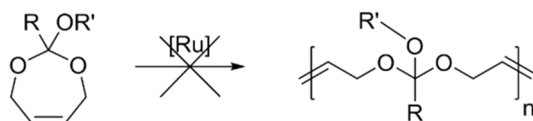
In comparison to the monomers, the corresponding ¹H NMR spectra show a shift of both the orthoester double bond

Scheme 3. (A) Synthesis of Cyclic Orthoester Monomers for ROMP (1–4), (B) ROMP Homopolymerization and (C) Copolymerization of Cyclic Orthoesters with 1,5-Cyclooctadiene and Subsequent Hydrogenation to Orthoester-Containing PE Mimics

A Monomer synthesis



B Homo polymerization



C Copolymerization and hydrogenation

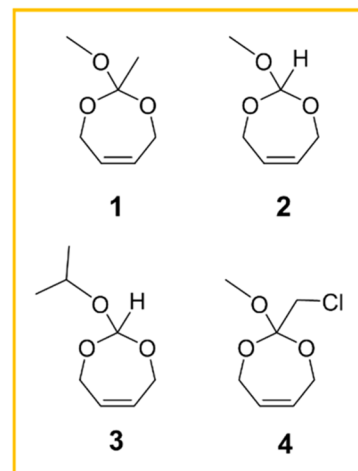
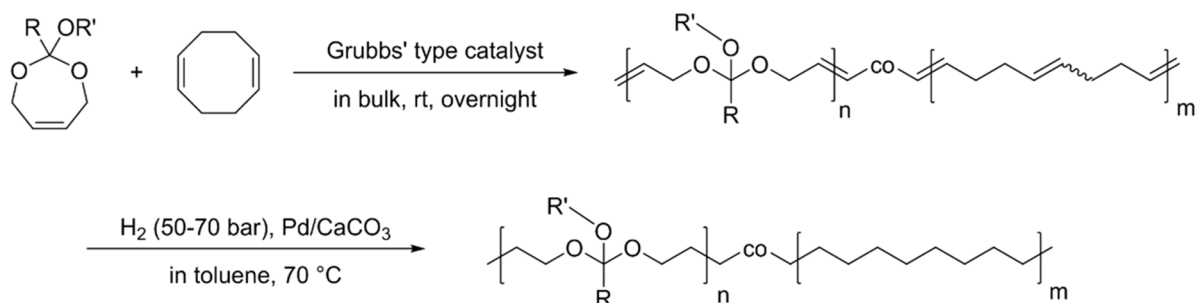


Table 1. Copolymerization of Orthoester Monomers 1–4 with Cyclooctadiene Using First-Generation Grubbs–Hoveyda Catalyst^a

monomer	ortho:COD feed	ortho:COD NMR ^d	M_n^c [g mol ⁻¹]	M_w^c [g mol ⁻¹]	M_n/M_w^c	yield [%]
1 ^b	1:1	1:2	900	1200	1.43	n.d.
1 ^b	1:2	1:3.5	1300	2000	1.61	n.d.
1 ^b	1:4	1:6.5	1700	3100	1.79	n.d.
2	1:1	1:2	10500	22500	2.14	60
2	1:2	1:4	11000	32200	2.95	83
2	1:4	1:6	15000	31000	2.60	n.d.
2 ^c	1:4	1:9	11600	30800	2.66	n.d.
3	1:1	1:2	5600	15000	2.75	47
3	1:2	1:3	8400	16600	1.99	65
3	1:4	1:5	11000	24000	2.20	77
3 ^c	1:4	1:9	10700	27300	2.54	75
4	1:1	1:2.5	6300	15300	2.42	n.d.
4	1:2	1:3.5	8900	24700	2.79	75
4	1:4	1:7	12700	38100	3.01	82

^aAll polymerizations were performed overnight at room temperature with first-generation Grubbs–Hoveyda catalyst (0.4 mol %) in bulk. ^b48 h polymerization time. ^cLarge-scale polymerization (>10 g). ^dDetermined by ¹H NMR. ^eDetermined by SEC.

and the $-O-CH_2$ group of the orthoester monomers to lower field (Figure 1). Overlapping poly-COD signals with slightly different chemical shifts elucidate the copolymer sequence as for poly(1)-*co*-COD, where the signal at 2.12 ppm corresponds to the $-CH_2$ group of a COD unit next to another COD unit, while the signal at 2.06 ppm indicates a neighboring orthoester unit. Additional information about the copolymer sequence is given by the signals corresponding to the polyorthoester double bonds: the signal at 5.72 ppm corresponds to an orthoester–COD dyad. The small signal at 5.90 ppm, however,

is giving a hint on an orthoester–orthoester dyad, even though the homopolymerization of 1 previously was not achieved.

By integration of the resonances of COD at 2.09 ppm and comparison to the orthoester resonances at 3.23 ppm, the relative ratio of orthoester to COD in the polymer was determined (indicated in the text by indices as in poly(1)₁-*co*-COD₂). The experimentally determined ratio is lower than the feed ratio since COD is the more reactive monomer during ROMP. The incorporation of orthoester units into the polymer chain was dependent on several factors: First, a lower amount

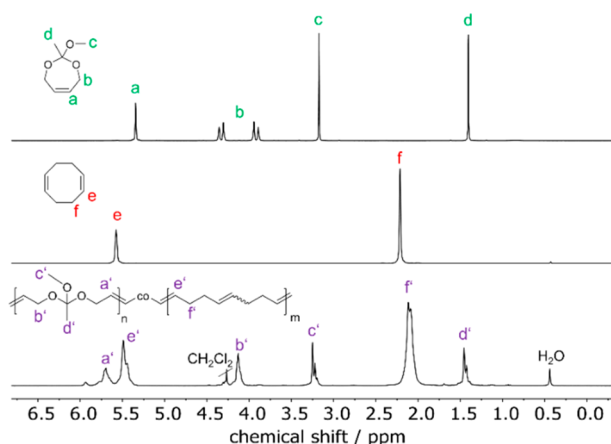


Figure 1. ^1H NMR (300 MHz at 298 K, in C_6D_6) of monomer 1 (top), cyclooctadiene (COD, middle), and the corresponding copolymer poly(1) $_1$ -*co*-COD $_2$ (bottom).

of initiator to monomers resulted in lower incorporation of the orthoester monomer (Table S1). Performing the polymerization in diluted conditions using THF as a solvent decreased the orthoester content in the copolymer in comparison to the polymerization in bulk. In terms of the initiator, the first-generation Grubbs–Hoveyda catalyst revealed the highest conversion of the orthoester monomers. The more active second-generation Grubbs–Hoveyda catalyst and third-generation Grubbs catalyst led to rapid consumption of COD, and no incorporation of 1–4 was detected. Increasing the amount of 1–4 in the monomer feed resulted in increased incorporations, however, always lower than the monomer feed ratio (20–65% lower than feed). When the copolymerizations of 2 and 3 with COD were performed at a larger scale (ca. 10 g), lower incorporations were obtained compared to the small scale reactions (200–400 mg).

Polymerizations were terminated by the addition of ethyl vinyl ether and isolated by precipitation into basic methanol (ca. 1 wt % of triethylamine were added to prevent hydrolysis). The polymers were recovered as brown viscous oils, indicating that the initiator could not be removed completely by simple precipitation. As the ROMP of COD produces linear poly(1,4-butadiene) with a mixture of *cis*- and *trans*-configured double bonds, crystallization of the polymer chains is hindered,³³ and all copolymers exhibited melting temperatures below room temperature (T_m maximum -9 °C).

To produce PE-like materials, we performed hydrogenation of the polymers with Pd on CaCO_3 in toluene at temperatures above 70 °C. Because of the high sensitivity of orthoesters toward hydrolysis in solution, the hydrogenation proved to be challenging. Despite using of anhydrous conditions and the addition of DIPEA (a soluble and relatively high-boiling amine base) certain hydrolysis of the orthoester functionality could not be prevented. Presumably, the remaining Grubbs' type catalyst could have caused the hydrolysis since HCl can be abstracted during the decomposition of the catalyst.³⁴ Especially the most sensitive poly(1)-*co*-COD (R = methyl) hydrolyzed rapidly. Furthermore, the solubility of the copolymers reduced drastically with ongoing hydrogenation, resulting in the copolymers being insoluble in toluene at room temperature. Thus, for purification the copolymers were dissolved in boiling toluene, the catalyst was filtered off while the solution was still hot, and the copolymers were

immediately precipitated into methanol containing DIPEA. The obtained off-white, solid materials were hard and partly brittle. The ^1H NMR spectrum of poly(3)-*co*-COD in toluene- d_8 (at 90 °C) proves the successful hydrogenation, as the resonances of the double bonds had disappeared completely, while an intense alkyl signal at 1.4 ppm indicates the presence of only methylene groups in the saturated polymer (Figure 2).

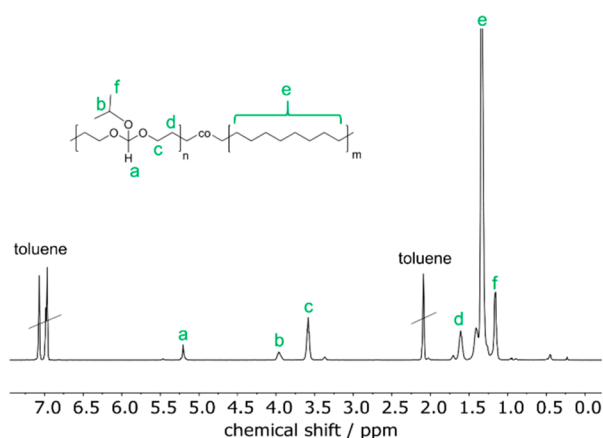


Figure 2. ^1H NMR (500 MHz at 353 K, in toluene- d_8) of hydrogenated copolymer poly(3) $_1$ -*co*-COD $_2$.

Solid-State Characterization. The non-hydrogenated poly(orthoester)-*co*-COD copolymers are honey-like, viscous oils, while the hydrogenated polymers are hard, solid materials. Yet, the hydrogenated copolymers were brittle, so we were unable to make a specimen for tensile strength tests. Possibly the molecular weights of the synthesized polymers were too low, as Gross and co-workers reported a brittle-to-ductile transformation for long-chain polyesters for an M_w between 53×10^3 and 78×10^3 g mol $^{-1}$.³⁵ The thermal stabilities of the copolymers were examined with thermal gravimetric analysis (TGA). The first derivative shows two main points of degradation (Figure S36), indicating that the orthoester and COD units degrade at different temperatures. For instance, hydrogenated poly(3) $_1$ -*co*-COD $_3$ has one main point of degradation at 343 °C and one at 475 °C (compared to 483 °C of HDPE). Furthermore, the weight loss after the first degradation process is dependent on the orthoester content in the copolymer (Figure 3A). For instance, the thermogram of hydrogenated poly(3) $_1$ -*co*-COD $_2$ reveals a weight loss of about 40% after the first degradation process, which matches the mol % of the orthoester monomers in the polymer. In general, the hydrogenated polymers are remarkably stable at elevated temperatures with an onset temperature (T_{on}) after 5% degradation for e.g. poly(3) $_1$ -*co*-COD $_5$ at 338 °C, which is about 100 °C below the measured T_{on} of HDPE. The non-hydrogenated copolymers decompose at lower temperatures in comparison to the related hydrogenated polymers (Figure 3B). As an example, T_{on} after 5% degradation for non-hydrogenated poly(3) $_1$ -*co*-COD $_5$ is 265 °C.

By differential scanning calorimetry (DSC), the melting points (T_m) and the crystallinity were determined. In most cases, a glass transition point was either not detectable or outside the measured range (minimum -100 °C). While the non-hydrogenated polymers are either amorphous or show a T_m below room temperature, the hydrogenated polymers have T_m up to 117 °C for poly(2) $_1$ -*co*-COD $_9$, which is similar to

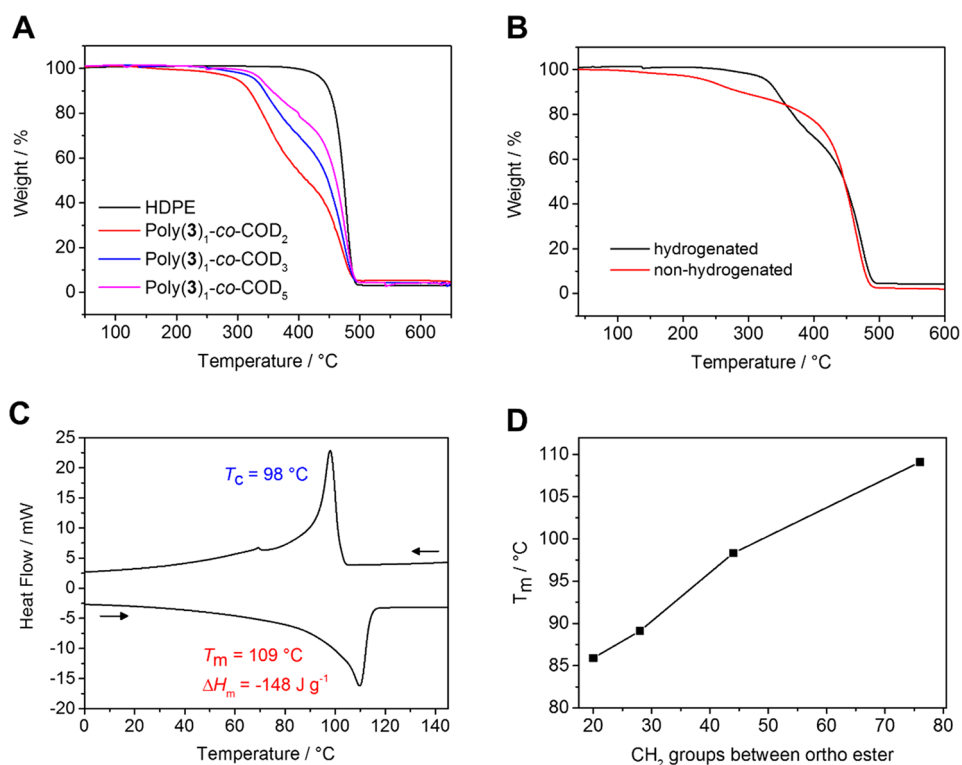


Figure 3. (A) TGA thermogram of hydrogenated poly(3)₁-co-COD₂, poly(3)₁-co-COD₃, poly(3)₁-co-COD₅, and HDPE. (B) TGA thermogram of hydrogenated (black) and non-hydrogenated (red) poly(3)₁-co-COD₃. (C) DSC thermogram of poly(3)₁-co-COD₉ (exo up, heating and cooling rate 10 K min⁻¹ (second run)). (D) Correlation of melting point T_m (from DSC) and the number of CH₂ groups between orthoester (by ¹H NMR) for poly(3)-co-COD.

completely linear PE with 134 °C⁶ (cf. Figure 3C shows the DSC thermogram of poly(3)₁-co-COD₉ with $T_m = 109$ °C). The melting enthalpies ΔH_m were between -84 and -162 J g⁻¹ and was compared to ΔH of 100% crystalline polyethylene ($\Delta H_m = 293$ J g⁻¹)³⁶ to calculate the crystallinity of the hydrogenated polymers. Both crystallinity and melting temperatures increased with increasing number of methylene groups between the orthoester groups, as the material becomes more similar to PE (cf. Table 2 and Figure 3D). The melting temperatures of our PE mimics start at ca. 86 °C for poly(3)₁-co-COD₂, which on average has 20 CH₂ groups between the orthoester groups (determined by ¹H NMR), and increase to 109 °C for poly(3)₁-co-COD₉ with on average 76 CH₂ groups as spacer (Figure 3D). Thus, with increasing COD amount in

the copolymer, the melting point of the hydrogenated polymers converges toward the value for PE.

The crystal structures of the three hydrogenated copolymers poly(2)₁-co-COD₉, poly(3)₁-co-COD₉, and poly(4)₁-co-COD₉ were compared to HDPE by XRD (Figure 4). A similar peak

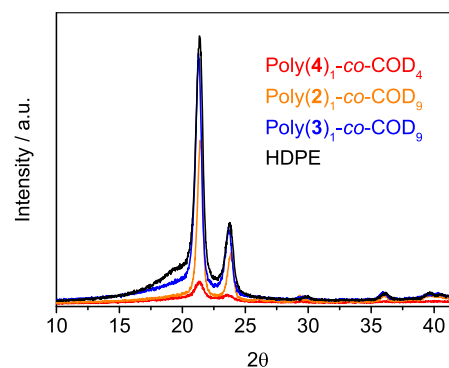


Figure 4. XRD diffractograms of hydrogenated poly(2)₁-co-COD₉, poly(3)₁-co-COD₄, and poly(4)₁-co-COD₉ and HDPE.

pattern in the X-ray diffractogram indicates an orthorhombic structure like HDPE in all three copolymer samples. The intensity of the peaks correlates with the degree of crystallinity.

The crystallization behavior of the orthoester–PE mimics was studied by drop-cast TEM measurements of solution grown crystals. Figure 5 shows a TEM micrograph of solution-grown crystals of hydrogenated poly(2)₁-co-COD₉, prepared from cooling a 0.05% solution of the polymer in *n*-octane to room temperature. The solution was heated to 70 °C in a temperature-controlled oil bath for 1 h and slowly cooled to

Table 2. Thermal Properties of Hydrogenated Copolymers

polymer	ortho:COD ^a	T_m^b [°C]	ΔH_m^b [J g ⁻¹]	crystallinity ^c [%]
poly(1)-co-COD	1:2	102	-156	53
poly(1)-co-COD	1:3.5	109	-167	57
poly(2)-co-COD	1:4.5	92	-116	39
poly(2)-co-COD	1:9	117	-163	55
poly(3)-co-COD	1:2	86	-84	29
poly(3)-co-COD	1:3	89	-93	32
poly(3)-co-COD	1:5	98	-95	33
poly(3)-co-COD	1:9	109	-148	51
poly(4)-co-COD	1:3.5	93	-86	29
poly(4)-co-COD	1:7	104	-116	40

^aDetermined by ¹H NMR. ^bDetermined by DSC. ^cRelative to 100% crystalline PE ($\Delta H_m = -293$ J g⁻¹).

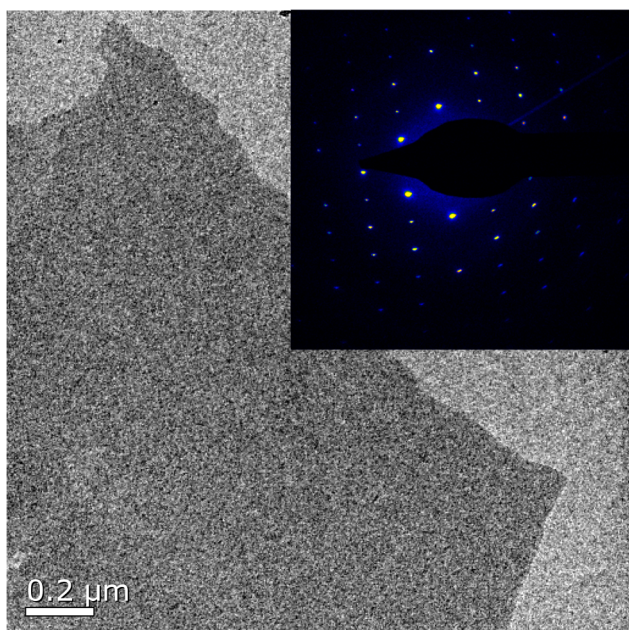


Figure 5. TEM bright-field micrograph and corresponding diffraction pattern (inset) of hydrogenated poly(2)₁-co-COD₉.

room temperature. One drop of this dispersion was applied to a carbon-coated TEM grid, excess liquid was blotted off with a filter paper, and the specimen was allowed to dry under ambient conditions. This preparation led to the formation of anisotropic polymer platelets with a thickness of only a few

nanometers and much higher lateral dimensions (Figure 5). Electron diffraction correlated to XRD data and reveals the single crystal pattern of flat-on orthorhombic PE crystals. All these polymers have similar crystal structure as common PE, and the introduction of orthoester defects into the PE main chain does not alter the crystal structure.

Moreover, the influence of defect frequency on lamellar thickness was studied using energy-filtered transmission electron microscopy (EFTEM) thickness mapping. Measurement of the crystals of hydrogenated poly(3)₁-co-COD₂ and poly(3)₁-co-COD₅ with an average number of CH₂ groups between ortho esters of 20 and 44, respectively, was carried out. This experiment revealed that the mean total lamellar thickness is ~3.7 nm for poly(3)₁-co-COD₂ and 9.8 nm for poly(3)₁-co-COD₅, demonstrating that randomly distributed orthoester groups along the polymer chain control the averaged thickness of PE-platelets; i.e., a decreased amount of orthoester groups resulted in an increased thickness of the polymer platelets. Furthermore, the mean total lamellar thickness for poly(3)₁-co-COD₂ was higher compared to the value for polyethylene with precise butyl branches at every 21st carbon (2.9 nm).⁹

Polymer Degradation. The degradation of polyorthoesters in acidic media occurs by hydrolysis to the corresponding alcohols and esters (Scheme 1). We varied the R' group to change the molecular structure of the degradation products. While the hydrolysis of poly(1)-co-COD, poly(2)-co-COD, and poly(4)-co-COD yields methanol, poly(3)-co-COD produces less toxic isopropanol. Furthermore, the substituent at the orthoester group has an influence on the hydrolysis rate:

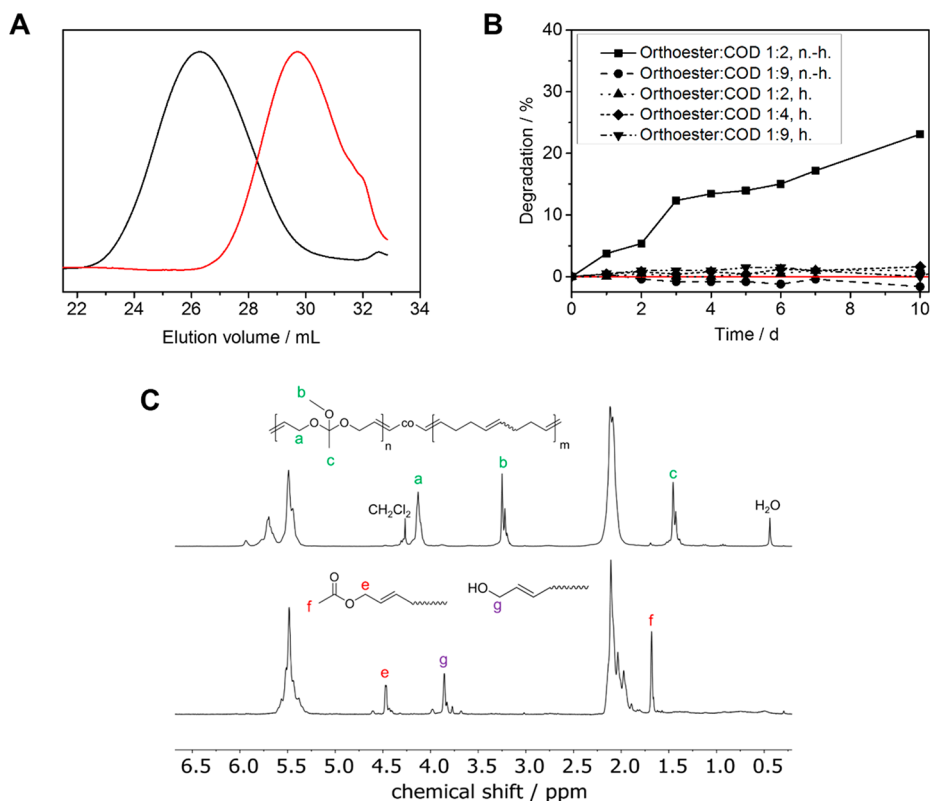


Figure 6. (A) SEC elugram (in THF) of poly(3)-co-COD before (black) and after degradation by hydrolysis (red). (B) Manometric respirometry biodegradation test of hydrogenated (h.) and non-hydrogenated (n.h.) poly(2)-co-COD using activated sludge from a local sewage plant. (C) ¹H NMR (300 MHz at 298 K, in C₆D₆) of poly(1)-co-COD (top) and after hydrolysis (bottom) with peak assignments.

von Delius and co-workers proved that relative to the electron density induced by the R-group hydrolysis the rate increases from $\text{CH}_2\text{Cl} < \text{H} < \text{Me}$.²⁶ Thus, our PE mimics were expected to exhibit an adjustable hydrolysis rate. In general, the unsaturated polymers exhibited shelf lives of below 6 months of storage (at room temperature under air), indicating hydrolysis of the honey-like materials from atmospheric moisture; the M_n of poly(3)-*co*-COD decreased from 8400 to 900 g mol^{-1} after storing the sample for 6 months without any precautions (Figure 6A). Comparing the ^1H NMR spectrum of poly(1)-*co*-COD directly after the synthesis with the spectrum after 6 months of storage, all corresponding orthoester signals had vanished completely (Figure 6C). Instead, peaks corresponding to the hydrolysis products (methyl ester and alcohol) were detected. We proceeded to examine the influence of the orthoester substituent on the hydrolytic degradation in a solution of the non-hydrogenated copolymers poly(1)-*co*-COD ($R = -\text{Me}$), poly(2)-*co*-COD ($R = -\text{H}$), and poly(4)-*co*-COD ($R = -\text{CH}_2\text{Cl}$). We performed these hydrolysis tests in *d*-THF and added 10 vol % of a solution of trifluoroacetic acid (TFA) in D_2O (i.e., 0.4 mol % TFA in relation to the orthoester). The reactions were monitored by ^1H NMR spectroscopy to determine the kinetic rate k and the half-life $t_{1/2}$ of hydrolysis. Our results were in agreement with the earlier findings of von Delius et al.²⁶ More electron-deficient orthoesters ($R = -\text{CH}_2\text{Cl}$, $t_{1/2} = 111$ h) were found to be more stable than orthoformates ($R = \text{H}$, $t_{1/2} = 10$ h), which in turn were found to be more stable than electron-rich orthoacetates ($R = \text{Me}$, $t_{1/2} = 3$ min) (Table 3).

Table 3. k and $t_{1/2}$ Values for Hydrolysis in *d*-THF with TFA in D_2O Observed by ^1H NMR at 298 K

polymer	substituent	k [s^{-1}]	$t_{1/2}$ [min]
poly(1) ₁ - <i>co</i> -COD ₂	–Me	3.8×10^{-3}	3
poly(2) ₁ - <i>co</i> -COD ₂	–H	1.9×10^{-5}	583
poly(4) ₁ - <i>co</i> -COD _{2,5}	–CH ₂ Cl	1.7×10^{-6}	6651

Polymer biodegradation studies in aerobic aqueous medium were performed according to the OECD 301F guideline for ready biodegradability using activated sludge from the local sewage treatment plant in Mainz, Germany, as the inoculum.³⁷ During this manometric respirometry test, the microorganism of the activated sludge converted the polymer to CO_2 under aerobic conditions. The CO_2 is trapped by KOH leading to a pressure decrease in the system. This pressure decrease can be measured and allows the calculation of the amount of biodegradation. For this test, we used an Oxitop setup and starch as the positive control. We tested three different copolymers: non-hydrogenated poly(3)₁-*co*-COD₂ and poly(3)₁-*co*-COD₉, the hydrogenated copolymers poly(3)₁-*co*-COD₂, poly(3)₁-*co*-COD₃ and poly(3)₁-*co*-COD₉ (Figure 6B). We followed literature procedures for biodegradation tests of hydrophobic compounds and doubled the amount of inoculum in comparison to the OECD guideline.³⁸ The surface of the polymers was increased prior to the test by emulsification (by ultrasound) of the oily non-hydrogenated polymers and by grinding of the solid hydrogenated polymer. The test was performed at a constant temperature of 20 °C. For the non-hydrogenated polymers, almost 25% of poly(3)₁-*co*-COD₂ was degraded after 10 days while no significant degradation of poly(3)₁-*co*-COD₉ was observed. Because of the aqueous media, we assume that first hydrolysis of the

copolymers occurs followed by the mineralization of the hydrolysis products (alcohols and esters) to CO_2 and H_2O by the microorganism. For fatty acid esters, the biodegradation rates decrease with increasing chain length.^{39,40} Because the hydrolysis products of poly(3)-*co*-COD are similar to them, this can explain the different biodegradability of poly(3)₁-*co*-COD₂ in comparison to poly(3)₁-*co*-COD₉. None of the hydrogenated polymers showed any biodegradability after 20 days. This can be explained by the increased hydrophobicity of the saturated polymers in comparison to the unsaturated polymers. However, the OECD 301F test aims to survey ready biodegradation (90% biodegradation within 30 days) and is optimized for water-soluble compounds. Thus, different long-term biodegradation tests for the long run have to be performed in the future to test the biodegradability of the synthesized orthoester copolymers. The fact that the ^1H NMR spectrum for the hydrogenated copolymers (e.g., poly(3)₁-*co*-COD₂, Figure S31) reveals hydrolysis after 6 months storage (at room temperature under air) suggests that further biodegradation is possible after this time.

3. EXPERIMENTAL SECTION

Materials. All commercially available reagents were purchased from Sigma-Aldrich, Alfa Aesar, Acros Organics, or TCI and were used without further purification unless otherwise stated. *cis*-2-Butene-1,4-diol was stored over dried 3 Å molecular sieves. Deuterated solvents were purchased from Sigma-Aldrich. All solvents were dried over molecular sieves for at least 24 h; chloroform-*d* was stored over anhydrous sodium carbonate, to quench residual acid, and activated 3 Å molecular sieves. Benzene-*d*₆ and toluene-*d*₈ were stored over activated 3 Å molecular sieves.

Instrumentation and Characterization Techniques. Size exclusion chromatography (SEC) measurements were performed in THF on an Agilent Technologies 1260 instrument consisting of an autosampler, a pump, and a column oven. The column set consists of three columns—SDV 10⁶ Å, SDV 10⁴ Å, and SDV 500 Å (PSS Standards Service GmbH, Mainz, Germany), all of 300 × 8 mm² and 10 μm average particle size—which were used at a flow rate of 1.0 mL/min and a column temperature of 30 °C. The injection volume was 100 μL. Detection was accomplished with an RI detector (Agilent Technologies). The data acquisition and evaluation were performed using PSS WINGPC UniChrom (PSS Polymer Standards Service GmbH, Mainz, Germany). Calibration was performed by using polystyrene provided by PSS Polymer Standards Service GmbH (Mainz, Germany). For nuclear magnetic resonance (NMR) analysis ^1H and ^{13}C NMR spectra of the monomers were recorded on a Bruker AVANCE III 300, 400, 500, or 700 MHz spectrometer. All spectra were measured in either CDCl_3 , C_6D_6 , toluene-*d*₈, or THF-*d*₈ at 298 K or in toluene-*d*₈ at 353 K. The spectra were calibrated against the solvent signal and analyzed using a MestReNova 12 from Mestrelab Research S.L. The thermal properties of the synthesized polymers have been measured by differential scanning calorimetry (DSC) on a Mettler Toledo DSC 823 calorimeter. Three scanning cycles of heating/cooling were performed in a nitrogen atmosphere (30 mL/min) with a heating and cooling rate of 10 °C/min. TGA was measured on a Mettler Toledo ThermoSTAR TGA/SDTA 851-Thermowaage in a nitrogen atmosphere. The heating rate was 10 °C/min in a range of temperature between 35 and 600–900 °C. Dynamic mechanical analysis (DMA) was performed using an Advanced Rheometric Expansion System (ARES) equipped with a force-balanced transducer. Plate/plate geometry was used with plate diameters of 6 mm. The gap between plates was around 1 mm. Experiments were performed under dry nitrogen atmosphere. The isochronal temperature dependencies of G' and G'' were determined for $\omega = 10$ rad/s. For wide-angle X-ray scattering (WAXS) experiments were performed using a Philips PW1820 powder diffractometer with Cu radiation (wavelength 1.5418 Å). The crystal

morphology, thickness, and crystal structure were determined using an FEI Tecnai F20 transmission electron microscope operated at an acceleration voltage of 200 kV. Bright-field (BF) and energy-filtered transmission electron microscopy (EFTEM) techniques were used for measurements. As solution-grown crystals lie flat-on on the supporting carbon film, their thickness was measured by EFTEM. The thickness estimation obtained from EFTEM was determined by

$$\frac{I_0}{I_t} = \exp\left(-\frac{t}{\lambda}\right)$$

where I_t is the total intensity of the inelastic spectrum energy, I_0 is the zeroth loss intensity of elastic spectrum energy, λ is the mean free path, and t is the thickness of the specimen. The relative thickness of the specimen t/λ can be directly determined by thickness mapping from EFTEM. The value of the mean free path λ depends on the composition of the specimen and on the convergence and collection semiangles of the TEM. Actually, the mean free paths of the carbon support, poly(3)_{1-co}-COD₂, and poly(3)_{1-co}-COD₃ were determined to $\lambda_C = 241$ nm, $\lambda_{\text{poly(3)-co-COD}_2} = 291$ nm, and $\lambda_{\text{poly(3)-co-COD}_3} = 294$ nm, respectively. The information contained in a thickness map image is the relative thickness t/λ and contains the superposition of the crystal lamellae and the supporting carbon film underneath. Accordingly, it is necessary to deconvolve these two in terms of thickness. It is easy to measure the thickness t_C of the carbon support alone. From the measured relative thickness t/λ of support and crystal it is then straightforward to calculate the crystal thickness t_{crystal} . For hydrolysis tests, 11–13 mg of each copolymer was dissolved in 550 μL of *d*-THF, and 50 μL of a 8.7×10^{-3} M TFA in D₂O solution was added directly before the start of the measurements. The hydrolysis reaction was monitored by ¹H NMR spectroscopy using a Bruker AVANCE III 500 spectrometer over a period of 2 h to 5 days. Biodegradation tests were performed using a WTW OxiTop IS 6 device. All bottles were equipped with a stirring bar, a rubber tubular charged with two pellets of KOH (to bind CO₂) and a measuring head. Activated sludge from the local sewage treatment plant in Mainz, Germany, was used as the inoculum. The activated sludge was aerated for 2 days prior to the biodegradation tests to minimize the residual organic content inside. All mineral media were prepared according to OECD guideline 301.³⁷ The inoculum was added without filtration to give an overall solid content of the inoculum of ca. 60 mg mL⁻¹. Between 27 and 34 mg of the test substances were added to each bottle to achieve a theoretical oxygen demand of about 80 mg L⁻¹. The oily, non-hydrogenated polymers were dispersed in the mineral medium and further ultrasonicated for 5 min prior to the addition to the bottles. Solid, hydrogenated polymers were grinded to minimize the particle size. Biodegradation tests were performed, in duplicate, over 30 days at a constant temperature of 20 °C. Starch was used as a positive control, and two bottles contained solely the inoculum and the mineral media to determine the blank value.

Synthetic Procedures. *Synthesis of 2-Chloro-1,1,1-trimethoxyethane.* 2-Chloro-1,1,1-trimethoxyethane was prepared according to the procedure reported by Moos et al.⁴¹

*General Experimental Procedure for the Synthesis of Cyclic Orthoester Monomers.*⁴² An oven-dried round-bottom flask equipped with a stirring bar was charged with orthoester (1.2 equiv) and *cis*-2-butene-1,4-diol (1 equiv). One drop of concentrated sulfuric acid was added to the reaction mixture under vigorous stirring. The reaction mixture was stirred at room temperature until all starting material was consumed (¹H NMR control) which took approximately 30–40 min. Anhydrous sodium carbonate (300 mg) was added to quench the acid. We noticed that too long reaction times can lead to the decomposition of the target compound. The reaction mixture was decanted and immediately distilled under reduced pressure (10⁻² bar) with a short Vigreux column to yield the desired monomers as colorless liquids. If necessary to obtain high purities, distillation was repeated several times.

2-Methoxy-2-methyl-4,7-dihydro-1,3-dioxepine (1). Yield: 22%. ¹H NMR (400 MHz, CDCl₃): δ 5.65 (t, $J = 1.7$ Hz, 2H), 4.38–4.45

(m, 2H), 4.16–4.10 (m, 2H), 3.34 (s, 1H), 1.51 (s, 3H). ¹³C NMR (101 MHz, CDCl₃): δ 128.79, 116.32, 61.39, 50.89, 18.26.

2-Methoxy-4,7-dihydro-1,3-dioxepine (2). Yield: 39%. ¹H NMR (400 MHz, CDCl₃): δ 5.71 (t, $J = 1.7$ Hz, 2H), 5.39 (s, 1H), 4.51–4.43 (m, 2H), 4.17–4.09 (m, 2H), 3.40 (s, 3 H). ¹³C NMR (101 MHz, CDCl₃): δ 129.15, 113.71, 61.51, 53.52.

2-Isopropoxy-4,7-dihydro-1,3-dioxepine (3). Yield: 66%. ¹H NMR (400 MHz, CDCl₃): δ 5.68 (t, $J = 1.8$ Hz, 1H), 5.55 (s, 1H), 4.50–4.43 (m, 2H), 4.13–4.07 (m, 2H), 3.96 (hept, $J = 8.3, 6.2$ Hz, 1H), 1.21 (d, $J = 6.3$ Hz, 6H). ¹³C NMR (101 MHz, CDCl₃): δ 129.20, 111.67, 68.45, 61.39, 22.57.

2-(Chloromethyl)-2-methoxy-4,7-dihydro-1,3-dioxepine (4). Yield: 75%. ¹H NMR (400 MHz, CDCl₃): δ 5.61 (t, $J = 1.8$ Hz, 2H), 4.46–4.39 (m, 2H), 4.19–4.12 (m, 2H), 3.66 (s, 2H), 3.34 (s, 3H). ¹³C NMR (101 MHz, CDCl₃): δ 128.30, 114.21, 61.94, 50.93, 39.98.

Representative Procedure for the Ring-Opening Metathesis Polymerization. The first-generation Grubbs–Hoveyda catalyst (5 mg) was charged in a 2 mL screw-top vial equipped with a stirring bar and flushed with argon before the vial was closed with a lid containing a septum. The respective orthoester monomer **2** (144 mg, 1.1 mmol) and 1,5-cyclooctadiene (239 mg, 2.2 mmol) were degassed by bubbling argon through the solution prior to the addition to the initiator via a syringe. The initiator quickly dissolved in the monomer mixture. The polymerization was conducted at room temperature and vigorous stirring. An increase in viscosity indicated the ongoing polymerization process. After 17 h, 1 mL of dichloromethane was added to dissolve the polymer, then 100 μL of ethyl vinyl ether to quench the polymerization, and 100 μL of trimethylamine to prevent hydrolysis. The mixture was further diluted with dichloromethane before precipitating from methanol containing a few droplets of trimethylamine. After centrifugation, the product was isolated and dried under reduced pressure to yield a brown, honey-like polymer. The ROMP polymers were obtained in 40–83% yield.

Poly(1)-co-COD. ¹H NMR (300 MHz, benzene-*d*₆): δ 5.72 (m, –O–CH₂–CH=), 5.48 (m, –CH₂–CH= (COD)), 4.13 (m, –O–CH₂–CH=), 3.23 (s, –O–CH₃), 2.09 (m, –CH₂–CH= (COD)), 1.44 (s, –C–CH₃). ¹³C NMR (75 MHz, benzene-*d*₆): δ 132.11, 129.73, 63.21, 49.71, 34.69–31.16 (m), 27.49, 20.19.

Poly(2)-co-COD. ¹H NMR (300 MHz, benzene-*d*₆): δ 5.65 (m, –O–CH₂–CH=), 5.57–5.35 (m, –CH₂–CH= (COD)), 5.27–5.17 (s, –CH), 4.20–4.00 (m, –O–CH₂–CH=), 3.23 (s, –O–CH₃), 2.09 (m, –CH₂–CH= (COD)). ¹³C NMR (75 MHz, benzene-*d*₆): δ 133.09, 130.04, 64.89, 50.74, 33.77–31.37 (m), 27.45.

Poly(3)-co-COD. ¹H NMR (300 MHz, benzene-*d*₆): δ 5.76–5.59 (m, –O–CH₂–CH=), 5.58–5.40 (m, –CH₂–CH= (COD)), 5.40–5.30 (s, –CH), 4.17 (m, –O–CH₂–CH=), 4.00 (m, –O–CH–(CH₃)₂), 2.10 (m, –CH₂–CH= (COD)), 1.16 (m, –O–CH–(CH₃)₂). ¹³C NMR (75 MHz, benzene-*d*₆): δ 130.36, 127.26, 67.18, 58.36, 38.40, 25.30, 23.76.

Poly(4)-co-COD. ¹H NMR (300 MHz, benzene-*d*₆): δ 5.65 (m, –O–CH₂–CH=), 5.58–5.34 (m, –CH₂–CH= (COD)), 4.20–3.96 (m, –O–CH₂–CH=), 3.50 (s, –CH₂–Cl), 3.18 (s, –O–CH₃), 2.09 (m, –CH₂–CH= (COD)). ¹³C NMR (75 MHz, benzene-*d*₆): δ 133.11, 130.45, 63.89, 50.24, 43.51, 33.25, 27.32.

Representative Procedure for Hydrogenation. The polymer (300 mg) was dissolved in 10 mL of dry toluene in a glass vessel, and the solution was degassed by bubbling argon through the solution for 15 min. 50 mg of 10 wt % Pd/CaCO₃ was added, and the glass vessel was charged into a 250 mL ROTH autoclave. Hydrogenation was performed at 70 °C and 70 bar of H₂. After completion of the reaction, hot toluene was added, and the hot reaction mixture was filtered and directly precipitated from cold methanol (containing NEt₃ to prevent hydrolysis). After centrifugation, the product was isolated and dried at reduced pressure to yield the polymer as an off-white powder. Yields were between 60% to quantitative yield.

Poly(1)-co-COD, Hydrogenated. ¹H NMR (500 MHz, toluene-*d*₈): δ 3.55 (m, –O–CH₂–CH₂–), 3.20 (s, –O–CH₃), 1.61 (m, –O–CH₂–CH₂–), 1.33 (b, alkyl backbone).

Poly(2)-co-COD, Hydrogenated. ^1H NMR (700 MHz, toluene- d_6): δ 5.05 (s, $-\text{CH}$), 3.36 (m, $-\text{O}-\text{CH}_2-\text{CH}_2-$), 3.21 (s, $-\text{O}-\text{CH}_3$), 1.59 (m, $-\text{O}-\text{CH}_2-\text{CH}_2-$), 1.52–1.09 (b, alkyl backbone).

Poly(3)-co-COD, Hydrogenated. ^1H NMR (500 MHz, toluene- d_6): δ 5.21 (s, $-\text{CH}$), 3.97 (m, $-\text{O}-\text{CH}-(\text{CH}_3)_2$), 3.75–3.46 (m, $-\text{O}-\text{CH}_2-\text{CH}_2-$), 1.76–1.52 (m, $-\text{O}-\text{CH}_2-\text{CH}_2-$), 1.34 (b, alkyl backbone), 1.18 (d, $-\text{O}-\text{CH}-(\text{CH}_3)_2$).

Poly(4)-co-COD, Hydrogenated. ^1H NMR (500 MHz, toluene- d_6): δ 3.73–3.55 (m, $-\text{O}-\text{CH}_2-\text{CH}_2-$), 3.53 (s, $-\text{CH}_2-\text{Cl}$), 3.24 (s, $-\text{O}-\text{CH}_3$), 1.68–1.52 (m, $-\text{O}-\text{CH}_2-\text{CH}_2-$), 1.36 (b, alkyl backbone).

4. SUMMARY

In this work, we report the synthesis of polyorthoesters by ring-opening metathesis polymerization (ROMP). Four different orthoester monomers were copolymerized with 1,5-cyclooctadiene (COD) in different ratios to yield unsaturated polymers with molecular weights up to 38000 g mol^{-1} . Postpolymerization hydrogenation gave hard, solid materials with thermal properties similar to polyethylene. The number of orthoester units in the polymer chain influenced thermal properties such as melting point or onset temperature of decomposition. Because of the brittle nature of the material, future work will focus on increasing the molecular weight of the long-chain polyorthoesters to better mimic the mechanical properties of polyethylene. Nevertheless, the biodegradability of the unsaturated orthoester copolymers represents a potential advantage when compared to polyethylene. All copolymers, hydrogenated and non-hydrogenated, hydrolyze slowly when exposed to atmospheric moisture. The hydrolysis rate in solution was found to be dependent on the orthoester substituent. In conclusion, long-chain polyorthoester copolymers are promising materials with the potential of replacing polyethylene for applications where a degradation over time is advantageous.

■ ASSOCIATED CONTENT

Supporting Information

The Supporting Information is available free of charge on the ACS Publications website at DOI: 10.1021/acs.macromol.9b00180.

Analytical and spectral characterization data as well as evaluation of biodegradation test (PDF)

■ AUTHOR INFORMATION

Corresponding Author

*E-mail wurm@mpip-mainz.mpg.de, Ph 0049 6131 379581, Fax 0049 6131 370 330 (F.R.W.).

ORCID

Ingo Lieberwirth: 0000-0003-1323-524X

Max von Delius: 0000-0003-1852-2969

Frederik R. Wurm: 0000-0002-6955-8489

Notes

The authors declare no competing financial interest.

■ ACKNOWLEDGMENTS

The authors thank the German Federal Ministry for Education and Research (BMBF) for their support of the program “Research for sustainable development (FONA)”, “PlastX – Plastics as a systemic risk for social-ecological supply systems” (grant 01UU1603A). O.Sh. and M.v.D. thank the University of Ulm and the German Research Foundation (DFG, Emmy-

Noether grant DE 1830/2-1) for financial support. O.Sh. is grateful for a doctoral scholarship by the German Academic Exchange Service (DAAD). We thank Michael Steiert (MPIP) for XRD measurements.

■ REFERENCES

- (1) Bioplastics market data 2017; <https://www.european-bioplastics.org/market/> (accessed 21.06.2018).
- (2) Malpass, D. B. *Introduction to Industrial Polyethylene: Properties, Catalysts, and Processes*; Wiley: 2010.
- (3) Haider, T. P.; Völker, C.; Kramm, J.; Landfester, K.; Wurm, F. R. Plastics of the Future? The Impact of Biodegradable Polymers on the Environment and on Society. *Angew. Chem., Int. Ed.* **2019**, *58* (1), 50–62.
- (4) Stempfle, F.; Ortmann, P.; Mecking, S. Long-Chain Aliphatic Polymers To Bridge the Gap between Semicrystalline Polyolefins and Traditional Polycondensates. *Chem. Rev.* **2016**, *116* (7), 4597–4641.
- (5) Trzaskowski, J.; Quinzler, D.; Bährle, C.; Mecking, S. Aliphatic Long-Chain C20 Polyesters from Olefin Metathesis. *Macromol. Rapid Commun.* **2011**, *32* (17), 1352–1356.
- (6) Ortmann, P.; Lemke, T. A.; Mecking, S. Long-Spaced Polyamides: Elucidating the Gap between Polyethylene Crystallinity and Hydrogen Bonding. *Macromolecules* **2015**, *48* (5), 1463–1472.
- (7) Ortmann, P.; Wimmer, F. P.; Mecking, S. Long-Spaced Polyketones from ADMET Copolymerizations as Ideal Models for Ethylene/CO Copolymers. *ACS Macro Lett.* **2015**, *4* (7), 704–707.
- (8) Steinbach, T.; Alexandrino, E. M.; Wahlen, C.; Landfester, K.; Wurm, F. R. Poly(phosphonate)s via Olefin Metathesis: Adjusting Hydrophobicity and Morphology. *Macromolecules* **2014**, *47* (15), 4884–4893.
- (9) Zheng, Y.-R.; Tee, H. T.; Wei, Y.; Wu, X.-L.; Mezger, M.; Yan, S.; Landfester, K.; Wagener, K.; Wurm, F. R.; Lieberwirth, I. Morphology and Thermal Properties of Precision Polymers: The Crystallization of Butyl Branched Polyethylene and Polyphosphoesters. *Macromolecules* **2016**, *49* (4), 1321–1330.
- (10) Ortmann, P.; Heckler, I.; Mecking, S. Physical properties and hydrolytic degradability of polyethylene-like polyacetals and polycarbonates. *Green Chem.* **2014**, *16* (4), 1816–1827.
- (11) Cordes, E. H. Mechanism and Catalysis for the Hydrolysis of Acetals, Ketals, and Ortho Esters. *Prog. Phys. Org. Chem.* **2007**, *4*, 1–44.
- (12) Binauld, S.; Stenzel, M. H. Acid-degradable polymers for drug delivery: a decade of innovation. *Chem. Commun.* **2013**, *49* (21), 2082–2102.
- (13) Heller, J. Synthesis of Biodegradable Polymers for Biomedical Utilization. *ACS Symp. Ser.* **1983**, *212*, 373–392.
- (14) Heller, J. In *Poly(ortho esters)*; Springer: Berlin, 1993; pp 41–92.
- (15) Heller, J.; Barr, J. Poly(ortho esters) From Concept to Reality. *Biomacromolecules* **2004**, *5* (5), 1625–1632.
- (16) Ng, S. Y.; Shen, H. R.; Lopez, E.; Zherebin, Y.; Barr, J.; Schacht, E.; Heller, J. Development of a poly(ortho ester) prototype with a latent acid in the polymer backbone for 5-fluorouracil delivery. *J. Controlled Release* **2000**, *65* (3), 367–374.
- (17) Wolfe, P. S.; Wagener, K. B. An ADMET route to unsaturated polyacetals. *Macromol. Rapid Commun.* **1998**, *19* (6), 305–308.
- (18) Khaja, S. D.; Lee, S.; Murthy, N. Acid-Degradable Protein Delivery Vehicles Based on Metathesis Chemistry. *Biomacromolecules* **2007**, *8* (5), 1391–1395.
- (19) Fraser, C.; Hillmyer, M. A.; Gutierrez, E.; Grubbs, R. H. Degradable Cyclooctadiene/Acetal Copolymers: Versatile Precursors to 1,4-Hydroxytelechelic Polybutadiene and Hydroxytelechelic Polyethylene. *Macromolecules* **1995**, *28* (21), 7256–7261.
- (20) Chikkali, S.; Stempfle, F.; Mecking, S. Long-Chain Polyacetals From Plant Oils. *Macromol. Rapid Commun.* **2012**, *33* (13), 1126–1129.

(21) Heller, J.; Barr, J.; Ng, S. Y.; Abdellauoi, K. S.; Gurny, R. Poly(ortho esters): synthesis, characterization, properties and uses. *Adv. Drug Delivery Rev.* **2002**, *54* (7), 1015–1039.

(22) Tschan, M. J.-L.; Jeong, N. S.; Todd, R.; Everson, J.; Dove, A. P. Unlocking the Potential of Poly(Ortho Ester)s: A General Catalytic Approach to the Synthesis of Surface-Erodible Materials. *Angew. Chem., Int. Ed.* **2017**, *56* (52), 16664–16668.

(23) Shyshov, O.; Brachvogel, R.-C.; Bachmann, T.; Srikantharajah, R.; Segets, D.; Hampel, F.; Puchta, R.; von Delius, M. Adaptive Behavior of Dynamic Orthoester Cryptands. *Angew. Chem., Int. Ed.* **2017**, *56* (3), 776–781.

(24) Brachvogel, R.-C.; Hampel, F.; von Delius, M. Self-assembly of dynamic orthoester cryptates. *Nat. Commun.* **2015**, *6*, 7129.

(25) Brachvogel, R.-C.; von Delius, M. Orthoester exchange: a tripodal tool for dynamic covalent and systems chemistry. *Chem. Sci.* **2015**, *6* (2), 1399–1403.

(26) Low, H.; Mena-Osteritz, E.; von Delius, M. Self-assembled orthoester cryptands: orthoester scope, post-functionalization, kinetic locking and tunable degradation kinetics. *Chem. Sci.* **2018**, *9*, 4785.

(27) Hilf, S.; Berger-Nicoletti, E.; Grubbs, R. H.; Kilbinger, A. F. M. Monofunctional Metathesis Polymers via Sacrificial Diblock Copolymers. *Angew. Chem., Int. Ed.* **2006**, *45* (47), 8045–8048.

(28) Steinbach, T.; Alexandrino, E. M.; Wurm, F. R. Unsaturated poly(phosphoester)s via ring-opening metathesis polymerization. *Polym. Chem.* **2013**, *4* (13), 3800–3806.

(29) Suthasupa, S.; Shiotsuki, M.; Sanda, F. Recent advances in ring-opening metathesis polymerization, and application to synthesis of functional materials. *Polym. J.* **2010**, *42*, 905.

(30) Hejl, A.; Scherman, O. A.; Grubbs, R. H. Ring-Opening Metathesis Polymerization of Functionalized Low-Strain Monomers with Ruthenium-Based Catalysts. *Macromolecules* **2005**, *38* (17), 7214–7218.

(31) Jung, M. E.; Piizzi, G. gem-Disubstituent Effect: Theoretical Basis and Synthetic Applications. *Chem. Rev.* **2005**, *105* (5), 1735–1766.

(32) Neary, W. J.; Kennemur, J. G. A Precision Ethylene-Styrene Copolymer with High Styrene Content from Ring-Opening Metathesis Polymerization of 4-Phenylcyclopentene. *Macromol. Rapid Commun.* **2016**, *37* (12), 975–979.

(33) Wagener, K. B.; Boncella, J. M.; Nel, J. G. Acyclic diene metathesis (ADMET) polymerization. *Macromolecules* **1991**, *24* (10), 2649–2657.

(34) Nelson, D. J.; Manzini, S.; Urbina-Blanco, C. A.; Nolan, S. P. Key processes in ruthenium-catalysed olefin metathesis. *Chem. Commun.* **2014**, *50* (72), 10355–10375.

(35) Liu, C.; Liu, F.; Cai, J.; Xie, W.; Long, T. E.; Turner, S. R.; Lyons, A.; Gross, R. A. Polymers from Fatty Acids: Poly(ω -hydroxyl tetradecanoic acid) Synthesis and Physico-Mechanical Studies. *Biomacromolecules* **2011**, *12* (9), 3291–3298.

(36) Busch, H.; Schiebel, E.; Sickinger, A.; Mecking, S. Ultralong-Chain-Spaced Crystalline Poly(H-phosphonate)s and Poly(phenylphosphonate)s. *Macromolecules* **2017**, *50* (20), 7901–7910.

(37) OECD Test No. 301: Ready Biodegradability, 1992.

(38) de Morsier, A.; Blok, J.; Gerike, P.; Reynolds, L.; Wellens, H.; Bontinck, W. J. Biodegradation tests for poorly-soluble compounds. *Chemosphere* **1987**, *16* (4), 833–847.

(39) Kleeberg, I.; Welzel, K.; VandenHeuvel, J.; Müller, R. J.; Deckwer, W. D. Characterization of a New Extracellular Hydrolase from *Thermobifida fusca* Degrading Aliphatic–Aromatic Copolyesters. *Biomacromolecules* **2005**, *6* (1), 262–270.

(40) Gerike, P. The biodegradability testing of poorly water soluble compounds. *Chemosphere* **1984**, *13* (1), 169–190.

(41) Moos, W. H.; Gless, R. D.; Rapoport, H. Codeine analogs. Synthesis of spiro[benzofuran-3(2H)4'-piperidines] and octahydro-1H-benzofuro[3,2-e]isoquinolines. *J. Org. Chem.* **1981**, *46* (25), 5064–5074.

(42) Pawlowski, C. Substituted 1,3-dioxepins. US3966768A, June 29, 1976.